Available online at www.sciencedirect.com
SCIENCE DIRECT®
Talanta 60 (2003) 377–393
Talanta
www.elsevier.com/locate/talanta

Logistic-exponential model for chemiluminescence kinetics

Bonawentura Kochel *

Department of Toxicology, Wrocław University of Medicine, 57/59 Traugutta St., PL-50417 Wrocław, Poland

Received 17 June 2002; received in revised form 6 November 2002; accepted 18 November 2002

Abstract

A logistic-exponential (LE) model for chemiluminescence (ChL) kinetics was constructed as a superposition of a logistic function, representing the ascending sigmoidal-in-shape phase, and an exponential function representing the descending phase of the ChL time course. The logistic component of the LE model expresses a non-linear autocatalytic reversible reaction counteracting a rise in the ChL which is not considered by a classical two-exponential model of the time course of ChL, whereas the exponential component of the LE model represents a first-order reaction of a ChL decay. The proposed reactions, that underlie the time course of ChL, were shown to form a second-order dynamic system. Main characteristics of the LE model such as the ChL peak value (CL_m), the peak time (t_m) and the inflexion points' times (t_i) were determined as well as the error calculus for the LE model. Moreover, several applications of the LE model to ChL processes generated by both native and perturbed polymorphonuclear granulocytes (PMNs) and red blood cells (RBCs), intoxicated yeast, ferrous ion-treated bull spermatozoa, autoxidising L-3,4-dihydroxyphenylalanine (L-DOPA), or luminol oxidised in the Fenton reaction were made.

Keywords: Chemiluminescence kinetics; Logistic-exponential model; Second-order dynamic systems

1. Introduction

A logistic-exponential (LE) model for ChL kinetics was built within the frames of the so called time-domain analysis [1], where a time course of a given process is the starting point for further analysis. This means that the LE model concerns, in the first place, a time course of ChL. The model was constructed in response to an inadequacy of a two-exponential model and a shortage of other proposals which have been seen for a few decades in this field. Since the main cause of that inadequacy lies in a discrepancy between the beginning phase of the two-exponential model and a sigmoidal form of the ascending phase of ChL, a construction of a new model was founded on a logistic function that reveals a desirable course.

A procedure of the construction of the LE model is presented here with a particular care which is necessary for new proposals, and because a differential equation, representing a superposition of infinitesimal forms of logistic and exponential processes, does not have, in general, a solution expressed by elementary functions. There-

* Fax: +48-71-344-4375.
E-mail address: kochel@pnet.pl (B. Kochel).

0039-9140/03/$ - see front matter
doi:10.1016/S0039-9140(03)00064-X

fore, a problem of approximation of this solution by elementary functions must be also solved. Moreover, a possibly simple form of the solution, being convenient for practical applications, must be determined.

Errors of the LE model were analysed, especially those produced by an estimation of the model's parameters on the basis of photon-counting time series representing the ChL time course, by simplification of the final form of the model, and due to the application of the model at small values of time (less than one-fifth of the ascending phase of ChL).

Several different examples of ChL (of PMN, RBCs, yeast, bull spermatozoa, L-DOPA, and luminol) were selected to demonstrate a wide spectrum of the LE model applications.

2. The logistic-exponential model

This section is consisted of four parts, in which: (1) a construction of the LE model is described; (2) two types of errors of the LE model are evaluated; (3) properties of the LE model are presented; and (4) a double logistic-exponential (DLE) model as a generalisation of the LE model, addressed to more complex ChL time courses, is given.

2.1. Construction of the model

Let an ascending sigmoidal phase of a time course of ChL be described by a logistic function:

$$\mathrm{CL}_{\mathrm{asc}}(t) = \frac{D}{1 + \exp(a + bt)}, \tag{1}$$

and let a descending phase of this process be a decay represented by an exponential function,

$$\mathrm{CL}_{\mathrm{des}}(t) = D \cdot \exp(-kt), \tag{2}$$

where the $a > 0$, $b < 0$, $k > 0$, $D > 0$ conditions were assumed owing to the experimental reasons.

Since a resulting velocity of the two component process is a sum of velocities of its components:

$$\frac{\mathrm{dCL}(t)}{\mathrm{d}t} = \frac{\mathrm{dCL}_{\mathrm{asc}}(t)}{\mathrm{d}t} + \frac{\mathrm{dCL}_{\mathrm{des}}(t)}{\mathrm{d}t}, \tag{3}$$

and $\mathrm{CL}_{\mathrm{des}}(t) \approx \mathrm{CL}(t)$, a differential equation representing the resulting process takes a form:

$$\frac{\mathrm{dCL}(t)}{\mathrm{d}t} = \frac{-D \cdot b \cdot \exp(a + bt)}{[1 + \exp(a + bt)]^2} - k \cdot \mathrm{CL}(t). \tag{4}$$

A solution of this equation has the following form:

$$\mathrm{CL}(t) = -b \cdot D \cdot \exp(-kt) \cdot \int \frac{\exp[a + (b + k)t]}{[1 + \exp(a + bt)]^2}\, \mathrm{d}t, \tag{5}$$

where the $\int \exp[a + (b + k)t)]/[1 + \exp(a + bt)]^2\, \mathrm{d}t$ integral is not an elementary function in general. The integration procedure applied to the $f(t) = \exp[a + (b + k)t)]/[1 + \exp(a + bt)]^2$ integrand, expanded in a Maclaurin series up to the fifth degree, i.e.

$$\int \frac{\exp[a + (b + k)t]}{[1 + \exp(a + bt)]^2}\, \mathrm{d}t \approx \int \sum_{n=0}^{5} \frac{f^{(n)}(0)}{n!}\, t^n \mathrm{d}t = \sum_{n=0}^{5} \frac{f^{(n)}(0)}{(n + 1)n!}\, t^{n+1}, \tag{6}$$

does not give a convergent approximation of the integral in general, as it is shown in Fig. 1 for $a = 1$, $b = -1$ and $k = 0.5$.

Integration by parts of the integral in Eq. (5) transforms it into a simpler form:

$$\int \frac{\exp[a + (b + k)t]}{[1 + \exp(a + bt)]^2}\, \mathrm{d}t = \frac{\exp(kt)}{b[1 + \exp(a + bt)]} - \frac{k}{b} \cdot \int \frac{\exp(kt)}{[1 + \exp(a + bt)]}\, \mathrm{d}t, \tag{7}$$

where $\int \exp(kt)/1 + \exp(a + bt)\, \mathrm{d}t$ is still not an elementary function, in general. To determine this integral its integrand $f(t) = \exp(kt)/1 + \exp(a + bt)$ was expanded in a Maclaurin series up to the fifth degree whereupon integrated:

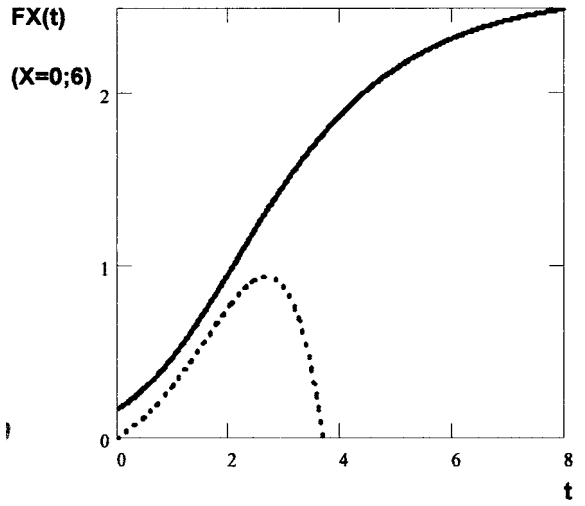

Fig. 1. The $\int \frac{\exp[a+(b+k)t]}{[1+\exp(a+bt)]^2}\,dt$ integral at $a=1$, $b=-1$ and $k=0.5$ is an elementary function of the form of $F0(t)=\frac{-\sqrt{e^t}}{1+e^{t-1}}+\sqrt{e}\cdot\arctan\sqrt{e^{t-1}}$ (Solid line). $F0(t)$ is not satisfactorily approximated in $[0,\infty)$ by the integrated expansion of the integrand described here by $F6(t)=\int\Sigma_{n=0}^{5}\frac{f^{(n)}(0)}{n!}t^n\,dt=\Sigma_{n=0}^{5}\frac{f^{(n)}(0)}{(n+1)n!}t^{n+1}$ (Dotted line).

$$\int \frac{\exp(kt)}{1+\exp(a+bt)}\,dt \approx \int \sum_{n=0}^{5}\frac{f^{(n)}(0)}{n!}\,t^n dt = \sum_{n=0}^{5}\frac{f^{(n)}(0)}{(n+1)n!}\,t^{n+1}. \quad (8)$$

This expansion, however, converges very slowly to $\int \exp(kt)/1+\exp(a+bt)\,dt$ as shown in Fig. 2 for $a=5$, $b=-1$ and $k=0.5$, where a satisfactory approximation is not obtained even for $n=5$, i.e. for F6(t), where the FN(t) symbol ($N=n+1$) stands for $\Sigma_{n=0}^{5}(f^{(n)}(0)/(n+1)n!)t^{n+1}$, although $\int(e^{t/2}/1+e^{5-t})dt$ is an elementary function: $F0(t)=2\sqrt{e^5}(\sqrt{e^{t-5}}-\arctan\sqrt{e^{t-5}})$.

At certain values of the a, b and k parameters the approximation of the integral based on the expansion into the Maclaurin series is a yet more ineffective as shown in Fig. 3. All the FN(t) functions considered here and F0(t) are divergent, i.e. the $|F0(t)-FN(t)|$ distance tends to infinity as

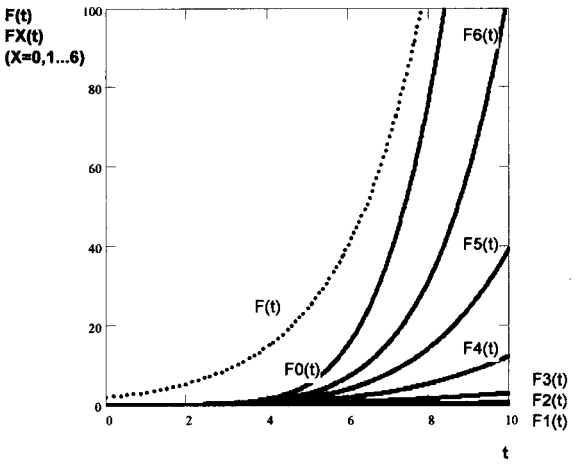

Fig. 2. Verification of the efficacy of the first few expansions F$N(t)$ ($N=1,2,\ldots,6$) approximating $\int\frac{\exp(kt)}{1+\exp(a+bt)}\,dt$ (symbolised here by F0(t)) at $a=5$, $b=-1$ and $k=0.5$. $F(t)=k^{-1}\exp(kt)$ majorizes the F0(t) and F$N(t)$ functions.

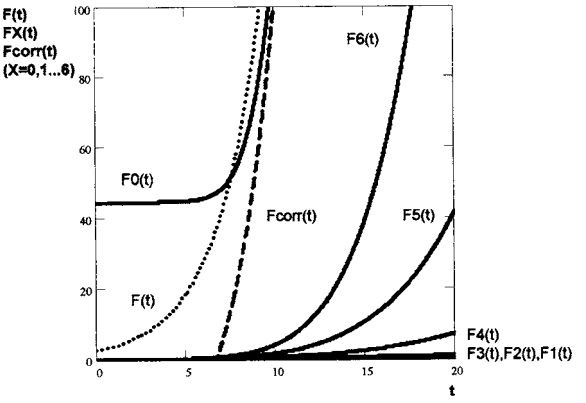

Fig. 3. Another verification of the efficacy of the first few expansions F$N(t)$ ($N=1,2,\ldots,6$) approximating $\int\frac{\exp(kt)}{1+\exp(a+bt)}\,dt$ (symbolised by F0(t)) at $a=8$, $b=-1$ and $k=0.4$. The F(t) function was corrected to $F_{corr}(t)=k^{-1}\exp(kt)-36.5$, which tends to F0($t$) as $t\to\infty$. The approximation inadequacy of the F$N(t)$ functions can be seen from from their graphs running away from F0(t) as $t\to\infty$. The F1(t) and F2(t) functions are not seen in this scale owing to their small values.

$t\to\infty$; only the $|F0(t)-F(t)|$ distance tends to a finite value of 36.5. At $\int\exp(kt)/1+\exp(a+bt)\,dt=F0(t)+c_o\cong F(t)+36.5$, where c_o is an integration constant, the $|F0(t)-F(t)|$ distance

obtains its explanation and the approximating function can be corrected to the form: $F(t)_{\mathrm{corr}} = k^{-1}\exp(kt) - c_{\mathrm{o}}$ which is valid for sufficiently large t values.

One can see from examples presented in Figs. 2 and 3 that $\int \exp(kt)/1 + \exp(a + bt)\,\mathrm{d}t$ may be approximated most effectively by $F_{\mathrm{corr}}(t) = k^{-1}\exp(kt) - c_{\mathrm{o}}$ (c_{o} is a constant), particularly when t takes sufficiently large values. The larger the time t the higher the efficacy of this approximation. Indeed, at $b < -k$ the integrand of the considered integral can be approximated by the function $\mathrm{F}(t) = \exp(kt)$ because of $\lim_{t\to\infty}(\exp(kt) - \exp(kt)/1 + \exp(a + bt)) = 0$. In consequence, this approximation together with Eq. (5) leads to a formula that is valid precisely for large values of t:

$$\mathrm{CL}(t) = D\left[\frac{1}{1 + \exp(a + bt)} - 1\right] + C\exp(-kt), \tag{9}$$

where the integration constant C can be calculated from the $\mathrm{CL}(0) = 0$ condition:

$$C = \frac{D}{1 + \exp(-a)}. \tag{10}$$

Finally,

$$\mathrm{CL}(t) = D\left[\frac{\exp(-kt)}{1 + \exp(-a)} - \frac{1}{1 + \exp(-a - bt)}\right]. \tag{11}$$

On the basis of the approximation used above, the formula given by Eq. (11) is valid for sufficiently large values of t. Therefore, in Eq. (11) rewritten as

$$\mathrm{CL}(t) = D\left[\frac{\exp(-kt) + \exp(bt)\{\exp(a)[\exp(-kt) - 1] - 1\}}{[1 + \exp(a + bt)]\,[1 + \exp(-a)]}\right], \tag{12}$$

one should include this fact in a reckoning, i.e.

$$\lim_{t\to\infty}(\exp(bt)\{\exp(a)[\exp(-kt) - 1] - 1\}) = 0, \tag{13}$$

which results in the following formulae useful in applications:

$$\mathrm{CL}(t) = \frac{D\exp(-kt)}{[1 + \exp(a + bt)]\,[1 + \exp(-a)]} \tag{14}$$

$$\mathrm{CL}(t) \cong \frac{D\cdot\exp(-kt)}{1 + \exp(a + bt)}, \tag{15}$$

the last of which is a particularly useful in practical applications when $\exp(-a) \approx 0$, i.e. when the value of $\exp(-a)$ can be neglected owing to sufficiently large values of the a parameter or due to the $\mathrm{CL}(t)$ measurement error.

Dimensions of the quantities occurring in Eq. (15) are as follows: $\dim(\mathrm{CL}(t)) = \dim(D) =$ the number of photoelectron counts recorded in a counting time Δt_{c}, $\dim(k) = 1/\dim(t)$, $\dim(a) = 0$, and $\dim(b) = 1/\dim(t)$, where $\dim(t)$ is the dimension of time used in the ChL measurement.

Readers not interested in details of error analysis can pass over Section 2.2 and go directly to Section 2.3 which is devoted to properties of the LE model.

2.2. Errors of the model

2.2.1. An error produced by small values of a

In order to determine the error resulting from the $\exp(-a) \approx 0$ assumption the following difference can be considered on the basis of Eqs. (14) and (15) as a definition of this error:

$$\Delta_{\mathrm{a}}\mathrm{CL}(t) := \frac{D\exp(-kt)}{1 + \exp(a + bt)} - \frac{D\exp(-kt)}{[1 + \exp(a + bt)]\,[1 + \exp(-a)]} = \frac{D\exp(-kt)}{1 + \exp(a + bt)}\left(\frac{1}{1 + \exp(a)}\right). \tag{16}$$

Then, the relative error of the $\mathrm{CL}(t)$ evaluation, being defined as $\delta_{\mathrm{a}}\mathrm{CL} := \{\Delta_{\mathrm{a}}\mathrm{CL}(t)/[\exp(-kt)/(1 + \exp(a + bt))]\} \times 100[\%]$, takes the following form depending only on the a parameter:

$$\delta_{\mathrm{a}}\mathrm{CL} = \frac{100}{1 + \exp(a)}\ [\%]. \tag{17}$$

Interpretation of $\delta_{\mathrm{a}}\mathrm{CL}$ results directly from the $\Delta\mathrm{CL}(t) > 0$ ($\Delta\mathrm{CL}(t) < 0$) inequality, and $\delta_{\mathrm{a}}\mathrm{CL} > 0$ ($\delta_{\mathrm{a}}\mathrm{CL} < 0$) means that the $\mathrm{CL}(t)$ value given by

Eq. (15) is overestimated (underestimated) and its value should be diminished (increased) by Δ_aCL. In practice (vide Section 4), when $a \in [2, 10]$ the δ_aCL value changes from 12 to 0.004%. If the CL(t) measurement error is greater than δ_aCL, this relative error (Eq. (17)) may be left out of account.

Of course, the use of a bit more complex model given in Eq. (14) (instead of that in Eq. (15)) is not connected with the errors considered above.

2.2.2. An error produced by small values of t

The model described by Eq. (15) was constructed without any assumptions regarding small values of t. Owing to the properties of $\int \exp(kt)/1+\exp(a+bt)\,dt$ it seems to be impossible to determine the general analytical relationship between the function corresponding to that integral and the a, b and k parameters occurring in the integrand. However, a suggestion on finding functions approximating the integral for small values of t can be inferred from Figs. 2 and 3. Consequently, an error produced by Eq. (15) for small values of t can be evaluated by considering a few simple functions presented in Figs. 2 and 3 corresponding to arbitrarily chosen a, b and k parameters. It has been verified that this choice of parameters does not limit the generality of the results obtained.

Therefore, let us consider a ChL process with the parameters: $a = 4.26$, $b = -1$ and $k = 0.2$. The $\int \exp(kt)/1+\exp(a+bt)\,dt$ integral (with the zero integration constant), presented in Fig. 4 by the $F(t)$ function, is parallel to the $F_1(t) = b^{-1}[a + bt - \ln(1+\exp(a+bt))]$ function in the time interval [0, 4]. Since a mean distance between the $F_1(t)$ and $F(t)$ functions, calculated according to the following definition,

$$\mathrm{d}(F_i(t),\ F_j(t)) := (T+1)^{-1}\sum_{t=0}^{T}|F_i(t)-F_j(t)|, \quad (18)$$

where $F_i(t)$ and $F_j(t)$ are two functions determined in the [0, T] interval, is equal to $\mathrm{d}(F(t), F_1(t)) = 2.13$ in the [0, 4] interval, and a variance of the $|F(t)-F1(t)|$ difference, corrected by that distance, i.e.

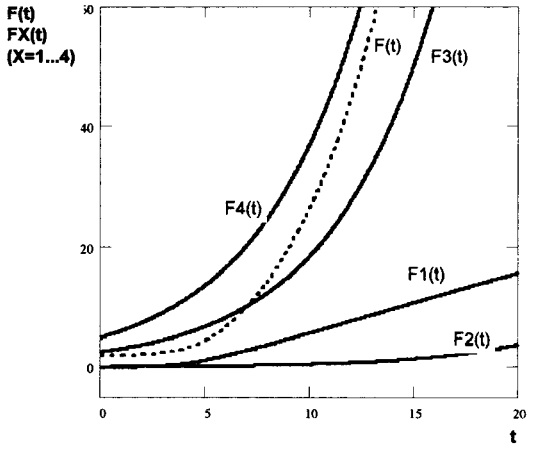

Fig. 4. The $\int \frac{\exp(kt)}{1+\exp(a+bt)}\,dt$ integral (represented by F(t)) is compared with the functions $F_1(t) = 1/b[a+bt-in(1+\exp(a+bt))]$, $F_2(t) = \exp(kt)/k[1+\exp(a)]$, $\mathrm{F}_3(t) = (2k)^{-1}$ - $\exp(kt)$ and $\mathrm{F}_4(t) = k^{-1}\exp(kt)$, at $a = 4.26$, $b = -1$ and $k = 0.2$, to find an approximation of its course at small values of t.

$$\sigma^2(F_i(t),\ F_j(t)):$$
$$= T^{-1}\sum_{t=0}^{T}[F_i(t)-F_j(t)-\mathrm{d}(F_i(t),\ F_j(t))]^2 \quad (19)$$

takes a minimum of 0.04 for the $(F(t),\ F_1(t))$ pair in comparison to the variances for other functions: $\sigma^2(F(t),\ F_2(t)) = 0.16$ at $\mathrm{d}(F(t), F_2(t)) = 2.22$, $\sigma^2(F(t),\ F_3(t)) = 12.80$ at $\mathrm{d}(F(t), F_3(t)) = 1.56$, or $\sigma^2(F(t),\ F_4(t)) = 151.92$ at $\mathrm{d}(F(t), F_4(t)) = 5.44$, a plot of the $\int \exp(kt)/1+\exp(a+bt)\,dt$ integral, at $a = 4.26$, $b = -1$ and $k = 0.2$, can be represented by $F1(t)+2.13$ in the [0, 4] time interval. Applying the procedure, already used in obtaining Eq. (12), one can educe the following $F_1(t)$ function-based formula valid for $t \le 4$:

$$\mathrm{CL}_{\mathrm{corr}}(t) = D\left\{\frac{1}{1+\exp(a+bt)}+\exp(-kt)\right.$$
$$\times\left[\frac{k}{b}\left(-bt+\ln\frac{1+\exp(a+bt)}{1+\exp(a)}\right)\right.$$
$$\left.\left.-\frac{1}{1+\exp(a)}\right]\right\}. \quad (20)$$

Let $\Delta_t\mathrm{CL}(t) := \mathrm{CL}(t)-\mathrm{CL}_{\mathrm{corr}}(t)$ stand for a deviation of CL(t) described by Eq. (15) from

$CL_{corr}(t)$ given in Eq. (20). Then, the relative error of the $CL(t)$ evaluation, i.e. $\delta_t CL(t) := \Delta_t CL(t)/CL(t)\cdot 100$ [%], takes positive (negative) values if the $CL(t)$ value is overestimated (underestimated) which means that $CL(t)$ should be diminished (increased) by $\delta_t CL(t)$. $\delta_t CL(t)$, contrary to $\delta_a CL$, depends on t. Depending on the a, b and k parameters $\delta_t CL(t)$ takes positive or negative values.

Several examples of the correction of the LE model at small values of time are presented in Figs. 5–7. The deviations between the LE model and its corrected versions take acceptable values. The computer programme MATHCAD 7 was found to be sufficient in fitting experimental data points by the LE model.

2.3. Properties of the model

There are three main quantities that characterise the LE model, namely a time moment (t_m) when the $CL(t)$ function reaches its peak value, the peak value itself (CL_m), and two time moments (t_{i1} and

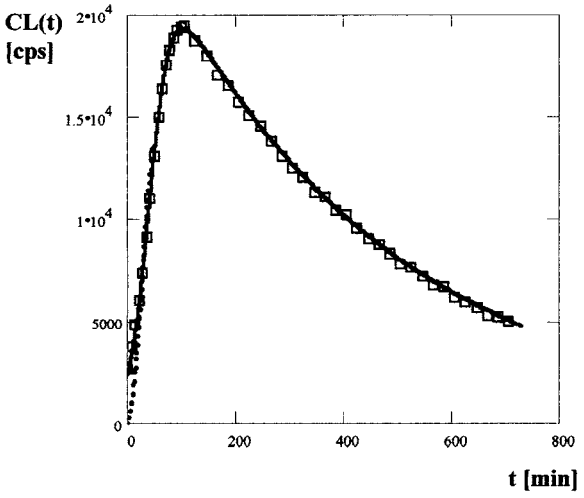

Fig. 5. ChL of DMSO-perturbed human PMNs stimulated with fMLP [2,3]. The experimental data points are fitted by the LE model of $CL(t) = 25\,655\exp(-0.0023t)/1+\exp(2.282-0.052t)$ in the whole time interval of the process (Solid line), whereas the corrected LE model $CL_{corr}(t) = 17113\exp(-0.0013t)/1+\exp(2.709-0.095t)$ fits these points in the interval of [0, 70] min (Dotted line).

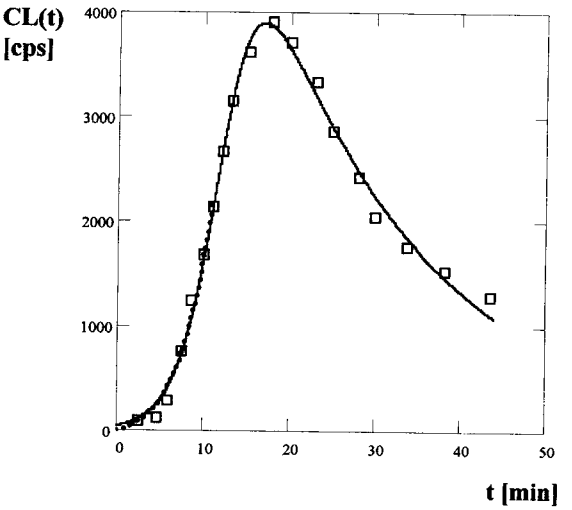

Fig. 6. ChL of L-DOPA autoxidation at pH 8.8 [4]. The time course in the whole time interval is modelled by $CL(t) = 10\,633\exp(-0.052t)/1+\exp(5.506-0.444t)$ (Solid line), and the course in the [0, 7] min interval is described by the corrected model $CL_{corr}(t) = 10394\exp(-0.046t)/1+\exp(5.008-0.348t)$ (Dotted line).

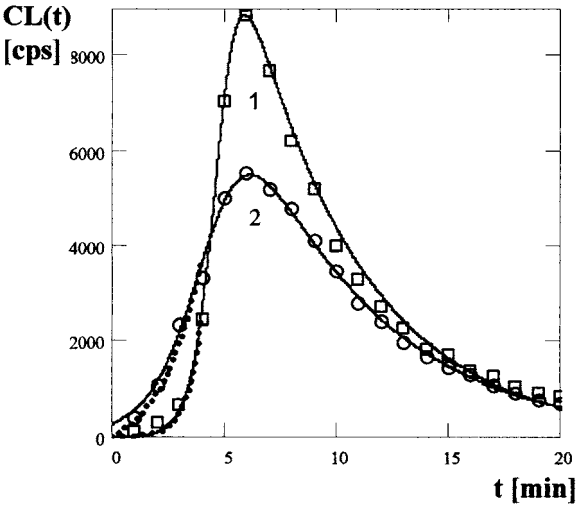

Fig. 7. ChL of Immax A-treated (1) or native (2) human RBCs initiated by t-BuOOH [5]. The LE models $CL(t) = 31\,300\exp(-0.196t)/1+\exp(9.260-1.938t)$ (1) or $CL(t) = 19295\exp(-0.171t)/1+\exp(4.264-0.935t)$ (2) describe the time course in the whole time interval (Solid lines), whereas the corrected models $CL_{corr}(t) = 30\,871\exp(-0.061t)/1+\exp(9.274-1.721t)$ (1) or $CL_{corr}(t) = 19\,943\exp(0.090t)/1+\exp(4.000-0.680t)$ (2) (Dotted lines) make this in the [0, 4] min interval.

t_{i2}) corresponding to two inflection points i_1 and i_2.

From the $dCL(t)/dt = 0$ condition, where $CL(t)$ is given in Eq. (15), an equation for t_m results:

$$t_m = \frac{1}{b}\cdot\left[\ln\left(\frac{-k}{b+k}\right) - a\right]. \tag{21}$$

A standard deviation of t_m is described by:

$$SD(t_m) = \sqrt{\left(\frac{SD(a)}{b}\right)^2 + \left(\frac{1}{b^2}\left[\ln\left(\frac{-k}{b+k}\right) - a\right] + \frac{1}{b(b+k)}\right)^2 SD^2(b) + \left(\frac{SD(k)}{k(b+k)}\right)^2} \tag{22}$$

where $SD(a)$, $SD(b)$ and $SD(k)$ are standard deviations of the a, b and k parameters, respectively.

The peak value of $CL(t)$ called here CL_m is defined as a $CL(t)$ value taken at $t = t_m$, i.e. $CL_m := CL(t_m)$:

$$CL_m = \frac{(b+k)D}{b} \cdot\exp\left\{\frac{-k}{b}\left[\ln\left(\frac{-k}{b+k}\right) - a\right]\right\}. \tag{23}$$

A standard deviation of CL_m has a form shown in Eq. (24):

$$SD(CL_m) = \frac{b+k}{b}\exp\left\{\frac{k}{b}\left[a - \ln\left(\frac{-k}{b+k}\right)\right]\right\} \cdot\sqrt{SD^2(D) + \left(\frac{kD}{b}\right)^2 SD^2(a) + \left\{\frac{D}{b}\left[a - \ln\left(\frac{-k}{b+k}\right)\right]\right\}^2 \cdot\left[\left(\frac{k}{b}\right)^2 SD^2(b) + SD^2(k)\right]}, \tag{24}$$

where $SD(D)$ is a standard deviation of the D parameter.

Two inflexion points i_1 and i_2, that occur at the ascending and descending phases, respectively, are characterised by the t_{i1} and t_{i2} time moments,

$$t_{i1/i2} = \frac{1}{b}\left[\ln\left(\frac{b^2 - 2k(b+k) \mp b\sqrt{b^2 - 4k(b+k)}}{2(b+k)^2}\right) - a\right], \tag{25}$$

which can be determined from the $d^2CL(t)/dt^2 = 0$ condition.

A standard deviation of t_{i1} is as follows:

$$SD(t_{i1}) = \sqrt{\left(\frac{\partial t_{i1}}{\partial a}\right)^2 SD^2(a) + \left(\frac{\partial t_{i1}}{\partial b}\right)^2 SD^2(b) + \left(\frac{\partial t_{i1}}{\partial k}\right)^2 SD^2(k)}, \tag{26}$$

where

$$\frac{\partial t_{i1}}{\partial a} = \frac{-1}{b}, \tag{27a}$$

$$\frac{\partial t_{i1}}{\partial b} = \frac{-1}{b^2}\left[\ln\left(\frac{Z(b,\,k)}{2(b+k)^2}\right) - a\right] + \frac{2(b+k)^2}{bZ(b,\,k)} \times\left[\frac{2(b-k) - Y(b,\,k) - (b^2 - 2bk)\cdot Y(b,\,k)}{2(b+k)^2}\right], \tag{27b}$$

$$Z(b,\,k) := b^2 - 2k(b+k) - bY(b,\,k)$$
$$Y(b,\,k) := \sqrt{b^2 - 4bk - 4k^2}, \tag{27c}$$

$$\frac{\partial t_{i1}}{\partial k} = \frac{2(b+k)^2}{bZ(b,\,k)}\left[\frac{-(b+2k)(1 - bY^{-1})}{(b+k)^2} - \frac{Z(b,\,k)}{(b+k)^3}\right]. \tag{27d}$$

A standard deviation of the a parameter, $SD(a)$, can be evaluated from a variance

$$SD(a) = \sqrt{\frac{1}{[t_m] - 1}\sum_{t=1}^{[t_m]}(\Delta a(t) - \langle\Delta a\rangle)^2}, \tag{28a}$$

of the $\Delta a(t)$ deviation:

$$\Delta a(t) := a(t) - a(t)_{\text{emp}}, \tag{28b}$$

produced by the difference between the empirical values $\text{CL}(t)_{\text{emp}}$ and those given by the $\text{CL}(t)$ model. $\langle \Delta a \rangle$ is a mean value of the deviation, i.e.

$$\langle \Delta a \rangle = \frac{1}{[t_{\text{m}}]} \sum_{t=1}^{[t_{\text{m}}]} \Delta a(t), \tag{28c}$$

and $[t_{\text{m}}]$ is an integer part of the peak time t_{m}.

The following holds:

$$\begin{aligned} \Delta a(t) &:= \ln\left(\frac{D\exp(-kt)}{\text{CL}(t)} - 1\right) \\ &\quad - \ln\left(\left|\frac{D\exp(-kt)}{\text{CL}(t)_{\text{emp}}} - 1\right|\right) \\ &= a - \ln\left(\left|\frac{D\exp(-kt)}{\text{CL}(t)_{\text{emp}}} - 1\right|\right) + bt, \end{aligned} \tag{28d}$$

since

$$\begin{aligned} \forall_{t\geq 0}\ a(t) &= \ln\left(\frac{D\exp(-kt)}{\text{CL}(t)} - 1\right) - bt = \text{const} \\ &= a. \end{aligned} \tag{28e}$$

Analogously, standard deviations of the b, k and D parameters can be determined from the following formulae:

$$\text{SD}(b) = \sqrt{\frac{1}{[t_{\text{m}}] - 1} \sum_{t=1}^{[t_{\text{m}}]} (\Delta b(t) - \langle \Delta b \rangle)^2}, \tag{29a}$$

$$\text{SD}(k) = \sqrt{\frac{1}{N - 1} \sum_{t=1}^{N} (\Delta k(t) - \langle \Delta k \rangle)^2}, \tag{29b}$$

$$\text{SD}(D) = \sqrt{\frac{1}{N - 1} \sum_{t=1}^{N} (\Delta D(t) - \langle \Delta D \rangle)^2}, \tag{29c}$$

at

$$\begin{aligned} \Delta b(t) &:= b(t) - b(t)_{\text{emp}} \\ &= b - \frac{1}{t}\left[\ln\left(\left|\frac{D\exp(-kt)}{\text{CL}(t)_{\text{emp}}} - 1\right|\right) - a\right], \end{aligned} \tag{30a}$$

$$\begin{aligned} \Delta k(t) &:= k(t) - k(t)_{\text{emp}} \\ &= k + \frac{1}{t} \\ &\quad \times \left[\ln\left(\frac{\text{CL}(t)_{\text{emp}}}{\text{CL}(t)_{\text{emp}}}(1 + \exp(a + bt))\right)\right], \end{aligned} \tag{30b}$$

and

$$\begin{aligned} \Delta D(t) &:= D(t) - D(t)_{\text{emp}} \\ &= D - \text{CL}(t)_{\text{emp}}\exp(kt) \\ &\quad \times [1 + \exp(a + bt)], \end{aligned} \tag{30c}$$

because of

$$\begin{aligned} \forall_{t\geq 0}\ b(t) &= \frac{1}{t}\left[\ln\left(\frac{D\exp(-kt)}{\text{CL}(t)} - 1\right) - a\right] = \text{const} \\ &= b, \end{aligned} \tag{31a}$$

$$\begin{aligned} \forall_{t\geq 0}\ \ k(t) &= \frac{-1}{t}\left[\ln\left(\frac{\text{CL}(t)(1 + \exp(a + bt))}{D}\right)\right] \\ &= \text{const} = k, \end{aligned} \tag{31b}$$

and

$$\begin{aligned} \forall_{t\geq 0}\ \ D(t) &= \text{CL}(t)\exp(kt)[1 + \exp(a + bt)] = \text{const} \\ &= D. \end{aligned} \tag{31c}$$

To illustrate the results of application of the above-mentioned formulae for the standard deviations of the LE model's parameters a few examples are presented below.

1) PMN + *N*-formylmethionyl-leucyl-phenylalanine (fMLP) [2]: $D \pm \text{SD}(D) = 39\,757 \pm 1139$ cps $\cong 40\,000 \pm 1200$ cps, $a \pm \text{SD}(a) = 3.085 \pm 0.059 \cong 3.09 \pm 0.06$, $b \pm \text{SD}(b) = -0.426 \pm 0.024\ \text{s}^{-1} \cong -0.43 \pm 0.03\ \text{s}^{-1}$, $k \pm \text{SD}(k) = 0.036 \pm 0.011\ \text{s}^{-1}$;
2) PMN + phorbol myristate acetate (PMA) [6]: $D \pm \text{SD}(D) = 2560 \pm 183$ cps, $a \pm \text{SD}(a) = 3.579 \pm 0.120 \cong 3.58 \pm 0.12$, $b \pm \text{SD}(b) = -0.334 \pm 0.086\ \text{min}^{-1} \cong -0.33 \pm 0.09\ \text{min}^{-1}$, $k \pm \text{SD}(k) = 0.045 \pm 0.060\ \text{min}^{-1}$;
3) PMN + cytochalasin B (CB) + PMA [6]: $D \pm \text{SD}(D) = 3442 \pm 237$ cps, $a \pm \text{SD}(a) = 3.190 \pm 0.124 \cong 3.19 \pm 0.13$, $b \pm \text{SD}(b) = -0.389 \pm 0.099\ \text{min}^{-1} \cong -0.39 \pm 0.10\ \text{min}^{-1}$, $k \pm \text{SD}(k) = 0.040 \pm 0.065\ \text{min}^{-1}$, where cps is count per second.

The relative standard error

$$SD_r(X) := \frac{SD(X)}{X}\ 100\ [\%], \tag{32}$$

of the LE model's parameters ($X = a, b, k, D$) in those experimental examples is as follows:

1) PMN+fMLP: $SD_r(D) \cong 3\%$, $SD_r(a) \cong 2\%$, $SD_r(b) \cong 7\%$, $SD_r(k) \cong 31\%$.
2) PMN+PMA: $SD_r(D) \cong 7\%$, $SD_r(a) \cong 3\%$, $SD_r(b) \cong 27\%$, $SD_r(k) \cong 133\%$.
3) PMN+CB+PMA: $SD_r(D) \cong 7\%$, $SD_r(a) \cong 4\%$, $SD_r(b) \cong 26\%$, $SD_r(k) \cong 144\%$.

Saying nothing of the evident fact that a measurement precision is different in different experiments, one can conclude that the experiments cited here allow one to evaluate almost precisely the a and D parameters, little worse the b parameter, and much less precisely the k parameter.

Since a precision of the LE model's characteristics depend on the precision of the LE model's parameters (Eqs. (22), (24) and (26)) the following evaluations hold true:

1) PMN+fMLP: $t_m \pm SD(t_m) = 12.835 \pm 0.984$ s $\cong 12.8 \pm 1.0$ s, $CL_m \pm SD(CL_m) = 22\,930 \pm 3359$ cps $\cong 23\,000 \pm 3400$ cps, $t_{i1} \pm SD(t_{i1}) = 6.500 \pm 0.415$ s $\cong 6.5 \pm 0.5$ s, $t_{i2} \pm SD(t_{i2}) = 19.169 \pm 1.593$ s $\cong 19.2 \pm 1.6$ s.
2) PMN+PMA: $t_m \pm SD(t_m) = 16.284 \pm 5.685$ min $\cong 16.3 \pm 5.7$ min, $CL_m \pm SD(CL_m) = 1065 \pm 1062$ cps, $t_{i1} \pm SD(t_{i1}) = 9.249 \pm 2.755$ min $\cong 9.2 \pm 2.8$ min, $t_{i2} \pm SD(t_{i2}) = 23.319 \pm 8.705$ min $\cong 23.3 \pm 8.7$ min.
3) PMN+CB+PMA: $t_m \pm SD(t_m) = 13.769 \pm 5.430$ s $\cong 13.8 \pm 5.5$ s, $CL_m \pm SD(CL_m) = 1780 \pm 1618$ cps, $t_{i1} \pm SD(t_{i1}) = 7.223 \pm 2.216$ min $\cong 7.2 \pm 2.3$ min, $t_{i2} \pm SD(t_{i2}) = 20.315 \pm 8.763$ min $\cong 20.3 \pm 8.8$ min.

A dependence of the CL(t) course on the a and b parameters is shown in Fig. 8.

The LE model's characteristics expressed in Eqs. (21), (23) and (25) are presented graphically in Fig. 9, whereas the model itself is compared with its logistic and exponential constituents or a two exponential model in Fig. 10.

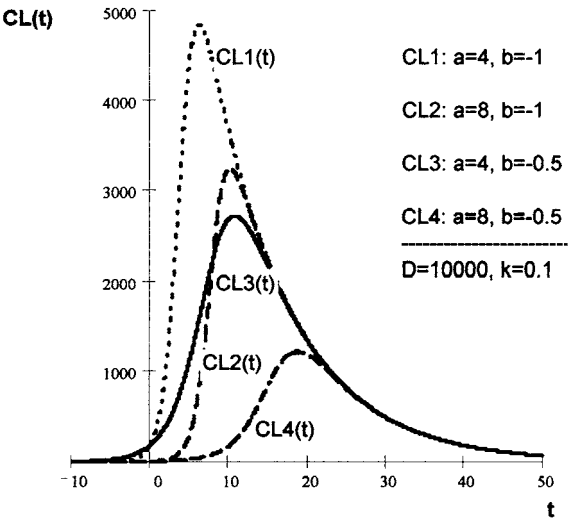

Fig. 8. Changes in the $CL(t) = D \exp(-kt)/1 + \exp(a + bt)$ function in dependence on the a and b parameters. An increase in the a value at b = constant results in a translation of the ascending phase and the peak time (t_m) to the larger values of t together with a reduction of the peak value (CL_m)) (CL1(t) vs. CL2(t)), whereas an increase in the b value at a = constant diminishes also the slope of the ascending phase (CL1(t) vs. CL3(t)). An increase both in the a and b values results in the above mentioned translation in time, the reduction in the peak value and the reduction of the slope (CL1(t) vs. CL4(t)). These cahnges are shown at the fixed k and D parameters. The descending phase is reduced by and increase either in the a or b parameters.

A dependence of the course of CL(t), described by the LE model, on the a or b parameters is shown in Figs. 11 and 12 as CL(a, t) or CL(b, t) functions.

2.4. The double logistic-exponential model

The LE model can be generalised to cover processes constituted from two parallel logistic processes composing the ascending phase of ChL. Such a model, which can be called as a DLE one, takes the form:

$$CL(t) = \frac{D \exp(-kt)}{[1 + \exp(a_1 + b_1 t)][1 + \exp(a_2 + b_2 t)]}. \tag{33}$$

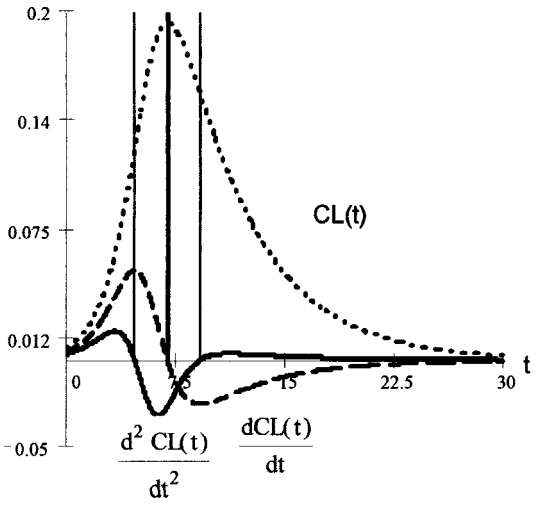

Fig. 9. Graphs of $CL(t) = D\exp(-kt)/1+\exp(a+bt)$ (Dotted line) and its 1st (Dashed line) and 2nd (Solid line) derivatives at $a = 5$, $b = -0.9$ a.u.$^{-1}$, $k = 0.2$ a.u.$^{-1}$ and $D = 1$ a.u. The peak value of $CL(t)$ corresponds to $t_m = 6.948$ a.u., the local maximum values of the 1st derivative or the zeros of the 2nd derivative indicate the time moments when the inflexion points occur: $t_{i1} = 4.686$ a.u. on the ascending branch and $t_{i2} = 9.209$ a.u. on the descending one. The a.u. stands for an arbitrary unit.

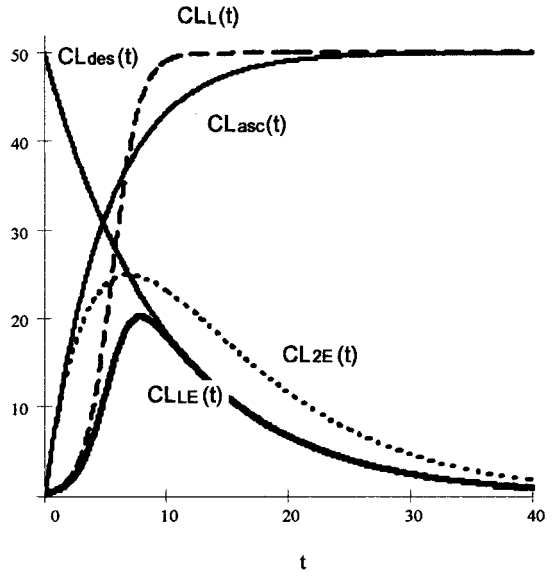

Fig. 10. Comparison of the classical exponential ($CL_{asc}(t) = D(1-\exp(-nt))$, ($CL_{des}(t) = D\exp(-kt)$), two exponential ($CL_{2E}(t) = (D\cdot n/k - n)[\exp(-nt) - \exp(-kt)]$) and logistic ($CL_L(t) = D/1+\exp(a+bt)$) models with the LE model ($CL_{LE}(t) = D\exp(-kt)/1+\exp(a+bt)$). The model's parameters $D = 50$, $n = 0.2$, $k = 0.1$, $a = 5$, $b = -0.9$, and time t are given in arbitrary units.

An example of the DLE model is presented in Fig. 13. This model competes with the LE model shown in the same figure, however, owing to the same accuracy in fitting the experimental data points, neither of these two models can be preferred. Probably, at a greater sampling frequency it would be possible to differentiate these two models, thus to verify a hypothesis about the existence of two different pathways of peroxide-generated excitation and transformation of luminol in the process of luminescence [7]. The LE, DLE and exponential models are compared in Fig. 14.

3. Mechanistic interpretation of the logistic-exponential model

On the basis of Eqs. (1) and (2) one can write the following system of equations respectively for the ascending (logistic) and descending (exponential) stages of the ChL process:

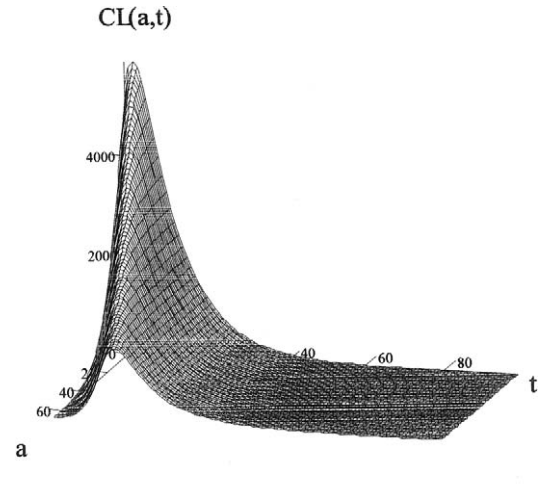

Fig. 11. Three dimensional surface representing ChL as a $CL(a, t)$ function at the b, k and D parameters fixed ($b = -0.5$, $k = 0.1$, $D = 10\,000$ given in arbitrary units).

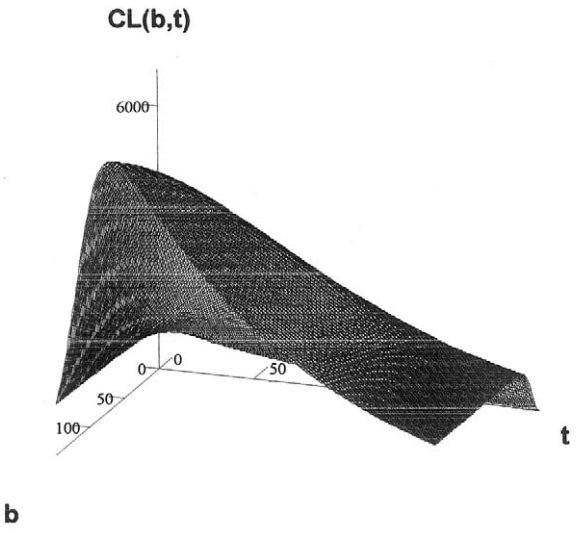

Fig. 12. Three dimensional surface representing ChL as a $CL(b,t)$ function at the a, k and D parameters fixed ($a=2$, $k=0.1$, $D=10\,000$ given in arbitrary units).

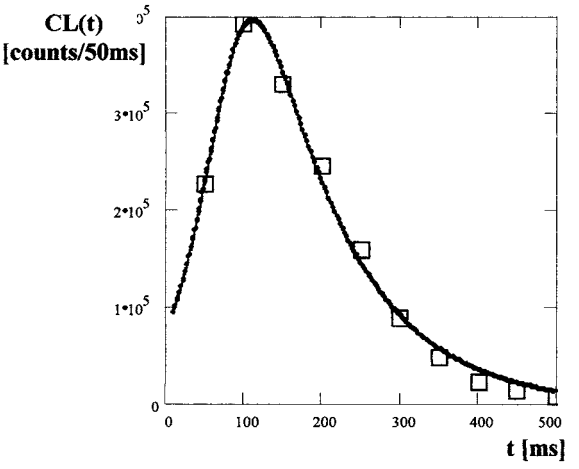

Fig. 13. The DLE model $CL(t)=1\ 505\ 800\exp(-0.0093t)/[1+\exp(2.942-0.036t)][1+\exp(3-0.7t)]$ (Dotted line) and the LE one $CL(t)=1\ 490\ 100\exp(-0.0093t)/[1+\exp(2.935-0.036t)]$ (Solid line) for ChL of luminol in the Fenton reaction [7] are indistinguishable one from another.

$$\frac{dCL_{asc}(t)}{dt} = -bCL_{asc}(t) + \frac{b}{D}\,CL^2_{asc}(t), \tag{34}$$

and

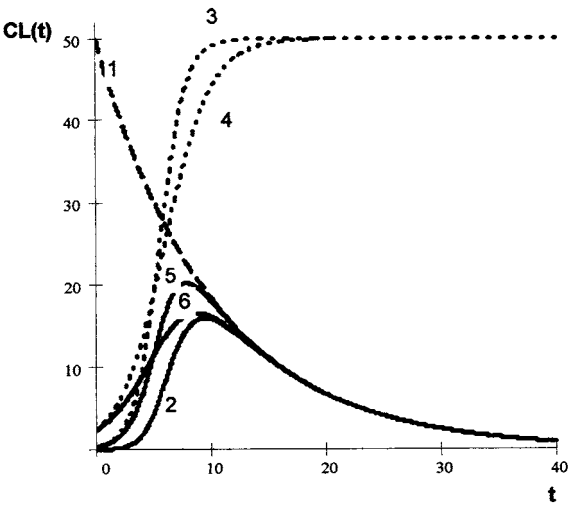

Fig. 14. Comparison of the DLE model ($CL_{DLE}(t)$; #2) with the exponential ($CL_{des}(t)$; #1), logistic ($CL_{L1}(t)$ and $CL_{L2}(t)$; #3 and 4) and LE models ($CL_{LE1}(t)$ and $CL_{LE2}(t)$; #5 and 6). The models' parameters $D=50$, $k=0.1$, $a_1=5$, $b_1=-0.9$, $a_2=3$ and $b_2=-0.5$ are given in arbitrary units. The function symbols are as follows:(1) $CL_{des}(t)=D\exp(-kt)$; (2) $CL_{DLE}(t)=D\exp(-kt)/[1+\exp(a_1+b_1\cdot t)][1+\exp(a_2+b_2\cdot t)]$; (3) $CL_{L1}(t)=D/[1+\exp(a_1+b_1\cdot t)]$; (4) $CL_{L2}(t)=D/[1+\exp(a_2+b_2\cdot t)]$;(5) $CL_{LE1}(t)=D\exp(-kt)/[1+\exp(a_1+b_1\cdot t)]$; (6) $CL_{LE2}(t)=D\exp(-kt)/[1+\exp(a_2+b_2\cdot t)]$.

$$\frac{dCL_{des}(t)}{dt} = -kCL_{des}(t), \tag{35}$$

where $b<0$, $k>0$ and $D>0$. Eq. (34) demonstrates that the exponential growth (because of $-b>0$) of the ChL, which is described by $dCL_{asc}(t)/dt=-bCL_{asc}(t)$, is diminished not only by the exponential decay (because of $-k>0$) given in Eq. (35) but additionally by the non-linear process: $dCL_{asc}(t)/dt=(b/D)CL^2_{asc}(t)$ (because of $b/D<0$).

The equation system given by Eqs. (34) and (35) means that a corresponding chemical system is a second-order dynamic one, where a dynamic variable $X(t)$ corresponds to $CL_{asc}(t)$ and another $Y(t)$ to $CL_{des}(t)$. From the proportionality between the ChL intensity, $CL(t)$, in a given time moment t, the concentration of various exited light-emitters or their intermediates $[A^*(t)]$, and the oxidant concentration $[Ox(t)]$:

$$CL(t) \sim [A^*(t)] \sim [Ox(t)], \tag{36}$$

one can interpret the $X(t)$ and $Y(t)$ variables as oxidants or emitters, and one can write the following reaction scheme

$$S + X \underset{k_{-1}}{\overset{k_1}{\rightleftarrows}} 2X; \quad X \underset{k_{-2}}{\overset{k_2}{\rightleftarrows}} Y; \quad Y \overset{k_3}{\rightarrow} P \ (h\nu), \tag{37}$$

describing a reversible autocatalytic reaction of generation of X followed by sequential reactions of transformation of X into Y, and the light-emitting decay of Y. S represents a reaction substrate and P is the measured reaction product, i.e. photons.

The postulate of the X↔Y reaction was necessary because the 1st-order system

$$\frac{d[X(t)]}{dt} = (k_1[S] - k_2)[X(t)] - k_{-1}[X(t)]^2, \tag{38}$$

corresponding to the following scheme,

$$S + X \underset{k_{-1}}{\overset{k_1}{\rightleftarrows}} 2X; \quad X \overset{k_2}{\rightarrow} P \quad (h\nu), \tag{39}$$

possesses a solution $X(t)$ which is only a logistic function.

The postulate of the X↔Y reaction, which resulted solely from the mathematical stipulation, seems to correspond with the hypothesis—formed on a purely chemical way—about the interaction between two radicals (X and Y) belonging to two different pathways of a luminol transformation during ChL [7], or the conclusion about the formation of two light-emitting compounds during the L-DOPA autoxidation reaction [4]. One can also find a correspondence with the radiationless transfer of energy from one excited molecule (X) to another (Y) which is followed by a radiation deactivation of the latter one [8].

The following system of differential equations corresponds to the scheme given in Eq. (37):

$$\frac{d[X(t)]}{dt} = (k_1[S] - k_2)[X(t)] - k_{-1}[X(t)]^2 + k_{-2}[Y(t)] \tag{40}$$

$$\frac{d[Y(t)]}{dt} = k_2[X(t)] - (k_3 + k_{-2})[Y(t)], \tag{41}$$

One can assume that $k_{-2}[Y(t)] \approx 0$ in Eqs. (40) and (41) because the experimental precision does not allow one to detect little deviations, expressed by the $k_{-2}Y(t)$ term, from the logistic curve of the form of $d[X(t)]/dt = (k_1[S] - k_2)[X(t)] - k_{-1}[X(t)]^2$. Moreover, at $k_3[Y(t)] \gg k_2[X(t)]$ the $k_2[X(t)]$ term in Eq. (41) exists without significant perturbation of the experimentally recorded exponential decay, given by $d[Y(t)]/dt = -k_3[Y(t)]$. These assumptions, i.e.

$$k_{-2}[Y(t)] \approx 0, \ \ k_3[Y(t)] \gg k_2[X(t)], \tag{42}$$

should be verified experimentally. At the present, however, the reaction system given in Eqs. (40)–(42) may be considered as the first approximation of mechanisms underlying ChL processes being described by the LE model.

The reaction rate constants can be determined from the LE model's parameters using Eqs. (34), (35), (40)–(42):

$$k_1[S] - k_2 = -b, \quad k_{-1} = \frac{-b}{D}, \quad k_3 = k. \tag{43}$$

If $k_1[S] - k_2 \geq 0$ then the 2nd-order system possesses two stationary non-negative states described by $d[X]/dt = 0$, namely: $[X]_1^* = 0$ and $[X]_2^* = k_1[S] - k_2/k_{-1} = D$, that are unstable or stable, respectively, and a single stationary state: $[Y]_1^* = 0$. This situation occurs for all empirical examples including those considered in Section 4. The situation of $k_1[S] - k_2 < 0$, at which there exists a single stationary state $[X]_1^* = 0$, is non-physical.

From Eq. (43) one can determine a linear effect of the generation of X described by $k_1[S] - k_2$ and a non-linear effect of the reduction of X expressed by k_{-1}. Contributions of the both effects into the whole reaction (described by Eq. (40) at Eq. (42)) can be evaluated as follows:

– a contribution of the linear effect of the X production (C_L^+):

$$C_L^+ := \frac{k_1[S] - k_2}{k_1[S] - k_2 + k_{-1}} \ 100 = \frac{100}{1 + 1/D} \ [\%] \tag{44}$$

– a contribution of the non-linear effect of the X reduction (C_{NL}^-):

$$C_{NL}^{-} := \frac{k_{-1}}{k_1[S] - k_2 + k_{-1}}\ 100 = \frac{100}{1 + D}\ [\%] \quad (45)$$

The contribution of the non-linear effect, though far smaller than the linear effect, is important because a sigmoidal shape of the ascending stage of ChL process occurs as its result. In the examples given in Section 4 C_{NL}^{-}does not exceed 0.2%.

In turn, the $(k_1[S]-k_2)/k_{-1} = D$ quotient describes an equilibrium of the X generation reaction (Eq. (40) at Eq. (42)).

The meaning of the inflexion points results from a difference in the ChL process in the time intervals between these points. At $t \le t_{i1}$ the oxidant generation rate raises with t to reach the maximum value at $t = t_{i1}$, then in $t_{i1} < t \le t_m$ the rate drops to zero at $t_{i1} = t_m$. At $t > t_m$ the oxidant decay dominates over the generation to reach the maximum value at $t = t_{i2}$ (Fig. 9). These features reveal an important role of the inflection points in choosing experimental conditions corresponding to the maximum value of the oxidant generation rate or that of the oxidant decay rate.

4. Applications of the logistic-exponential model

ChL processes presented below are various examples of the application of the proposed LE model. Amongst the eight examples presented here there are phagocyte luminescence produced by DMSO- or CB-treated human PMNs stimulated with fMLP or PMA, luminescence of PMNs phagocytosing opsonised zymosan (OZ), ChL of Immax A-treated RBCs during a homolytic scission of *tert*-butyl hydroperoxide (*t*-BuOOH), ChL of formaldehyde (HCHO)-perturbed yeast, ChL of the autoxidative reaction of L-DOPA, ferrous ion-induced ChL of bull spermatozoa, and ChL of luminol oxidised in the Fenton reaction. For all these processes the parameters of the LE model were determined as well as basic characteristics such as t_m, CL_m and t_{i1}, t_{i2} were calculated. Moreover, the reaction rate constants were evaluated from the model parameters. In those examples, in which a comparison of the models for perturbed biosystems with those for unperturbed ones was possible, the effects exerted by perturbers were evaluated on a basis of the constructed models.

In figures, the experimental data points are fitted by the LE model with the D, a, b and k parameters given in tables, where the basic characteristics of the considered ChL processes are also presented. In other tables some parameters of the postulated reactions corresponding to the particular LE models are shown.

4.1. Chemiluminescence of native and DMSO-perturbed isolated human PMNs stimulated with fMLP

Quenching of phagocyte luminescence by DMSO was described on the occasion of constructing the photon-counting process-based stochastic measures of homeostasis perturbation [9] and xenobiotic toxicity [2,3] as well as biphasic modulation of phagocytosis [10]. Time courses of ChL of isolated DMSO-perturbed (21 mM) or native human PMNs (10^5 cells ml^{-1}) stimulated with fMLP (1 μM) in the presence of luminol (2.5

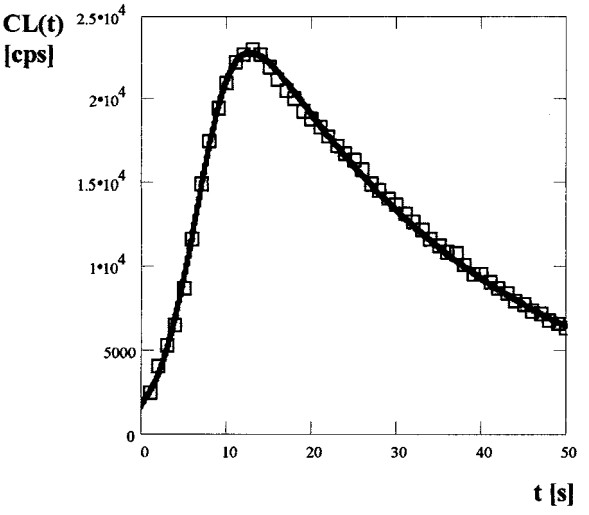

Fig. 15. The LE model for ChL of human PMNs stimulated with fMLP [2]:$CL(t) = 39757\exp(-0.036t)/1 + \exp(3.085 - 0.426t)$.

Table 1
Parameters and basic characteristics of the LE model for chemiluminescence of the analysed systems

System\parameter	D	A	b	k	t_m	CL_m	t_{i1}	t_{i2}
PMNs+fMLP+luminol	39 757 cps	3.085	$-0.426\ s^{-1}$	$0.036\ s^{-1}$	12.8 s	22 930 cps	6.5 s	19.2 s
PMNs+fMLP+DMSO+luminol	25 655 cps	2.282	$-0.052\ s^{-1}$	$0.0023\ s^{-1}$	103.0 s	19 349 cps	40.6 s	165.4 s
PMNs+PMA+luminol	2560 cps	3.579	$-0.334\ s^{-1}$	$0.045\ s^{-1}$	16.3 s	1065 cps	9.3 s	23.3 s
PMNs+PMA+CB+luminol	3442 cps	3.190	$-0.389\ s^{-1}$	$0.040\ s^{-1}$	13.8 s	1780 cps	7.2 s	20.3 s
PMNs+OZ	538 cps	3.790	$-1.345\ min^{-1}$	$0.043\ min^{-1}$	5.4 min	414 cps	2.7 min	8.0 min
PMNs+OZ+luminol	3033 cps	4.356	$-0.990\ min^{-1}$	$0.086\ min^{-1}$	6.8 min	1546 cps	4.1 min	9.5 min
RBCs+t-BuOOH+luminol	19 295 cps	4.264	$-0.935\ min^{-1}$	$0.171\ min^{-1}$	6.2 min	5497 cps	3.9 min	8.5 min
RBCs+t-BuOOH+Immax A+luminol	31 300 cps	9.260	$-1.938\ min^{-1}$	$0.196\ min^{-1}$	5.9 min	8842 cps	4.6 min	7.2 min
L-DOPA at pH 8.8	10 663 cps	5.506	$-0.444\ min^{-1}$	$0.052\ min^{-1}$	17.0 min	3899 cps	11.4 min	22.5 min
L-DOPA at pH 8.6	5118 cps	5.759	$-0.221\ min^{-1}$	$0.021\ min^{-1}$	36.3 min	2163 cps	24.5 min	48.1 min
Yeast+HCHO	2804 cps	2.746	$-0.055\ s^{-1}$	$0.0035\ s^{-1}$	98.8 s	1858 cps	45.5 s	152.1 s
Spermatozoa+Fe^{++}	3716 cps	4.645	$-0.355\ s^{-1}$	$0.030\ s^{-1}$	19.8 s	1878 cps	12.2 s	27.4 s
Luminol+H_2O_2+Fe^{++}	1 490 100 c/50 ms	2.935	$-0.036\ ms^{-1}$	$0.0093\ ms^{-1}$	110.8 ms	397 289 c/50 ms	56.5 ms	165.2 ms

μM) are shown in Figs. 5 and 15, respectively. The parameters and basic characteristics of the LE model are given as well as chemical reactions corresponding to this model are presented in Tables 1 and 2.

The ChL quenching is seen directly from: (a) the reduced CL_m value; (b) the heightened t_m value; and (c) the heightened t_{i1} and t_{i2} values. Comparison of the model parameters for native and DMSO-perturbed PMNs allows one to evaluate quantitatively effects exerted by DMSO on the light-emitter or oxidant generation during phagocytosis. The D value is diminished by 35.5% due to DMSO, which-owing the $(k_1[S]-k_2)/k_{-1}=D$ relationship-means that the reaction in Eq. (40) is shifted to the left side, i.e. to the decreased

Table 2
Parameters of the reactions corresponding to the LE model for chemiluminescence of the analysed systems

System\parameter	$k_1[S]-k_2$	k_{-1}	k_3	C_L^+ (%)	C_{NL}^- (%)
PMNLs+fMLP+luminol	$0.426\ s^{-1}$	$10^{-5}\ s^{-1}$	$0.036\ s^{-1}$	99.997	0.003
PMNLs+fMLP+DMSO+luminol	$0.052\ s^{-1}$	$0.2\times10^{-5}\ s^{-1}$	$0.0023\ s^{-1}$	99.996	0.004
PMNLs+PMA+luminol	$0.334\ s^{-1}$	$1.30\times10^{-4}\ s^{-1}$	$0.045\ s^{-1}$	99.961	0.039
PMNLs+PMA+CB+luminol	$0.389\ s^{-1}$	$1.13\times10^{-4}\ s^{-1}$	$0.040\ s^{-1}$	99.971	0.029
PMNLs+OZ	$1.345\ min^{-1}$	$25.0\times10^{-4}\ min^{-1}$	$0.043\ min^{-1}$	99.814	0.186
PMNLs+OZ+luminol	$0.990\ min^{-1}$	$3.26\times10^{-4}\ min^{-1}$	$0.086\ min^{-1}$	99.967	0.033
RBCs+t-BuOOH+luminol	$0.935\ min^{-1}$	$4.84\times10^{-5}\ min^{-1}$	$0.171\ min^{-1}$	99.995	0.005
RBCs+t-BuOOH+Immax A+luminol	$1.938\ min^{-1}$	$6.19\times10^{-5}\ min^{-1}$	$0.196\ min^{-1}$	99.997	0.003
L-DOPA at pH 8.8	$0.444\ min^{-1}$	$4.16\times10^{-5}\ min^{-1}$	$0.052\ min^{-1}$	99.991	0.009
L-DOPA at pH 8.6	$0.221\ min^{-1}$	$4.32\times10^{-5}\ min^{-1}$	$0.021\ min^{-1}$	99.980	0.020
Yeast+HCHO	$0.055\ s^{-1}$	$1.96\times10^{-5}\ s^{-1}$	$0.0035\ s^{-1}$	99.964	0.036
Spermatozoa+Fe^{++}	$0.355\ s^{-1}$	$9.55\times10^{-5}\ s^{-1}$	$0.030\ s^{-1}$	99.973	0.027
Luminol+H_2O_2+Fe^{++}	$0.036\ ms^{-1}$	$2.42\times10^{-8}\ ms^{-1}$	$0.009\ ms^{-1}$	99.999933	6.7×10^{-5}

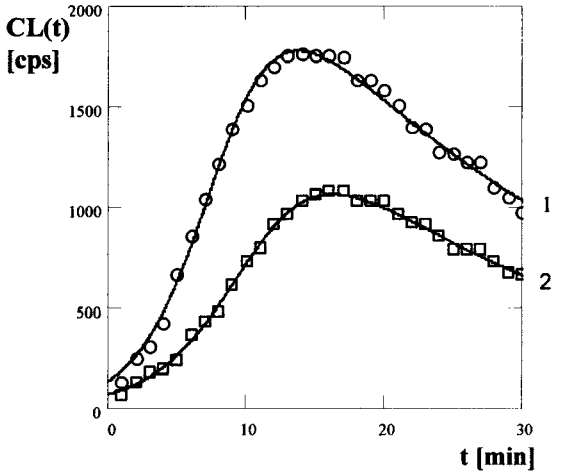

Fig. 16. The LE models for ChL of human CB-treated (1) or native (2) PMNs stimulated with PMA [6];(1) $CL(t) = 3442\ \exp(-0.040t)/1 + \exp(3.190 - 0.389t)$,(2) $CL(t) = 2560\ \exp(-0.045t)/1 + \exp(3.579 - 0.334t)$.

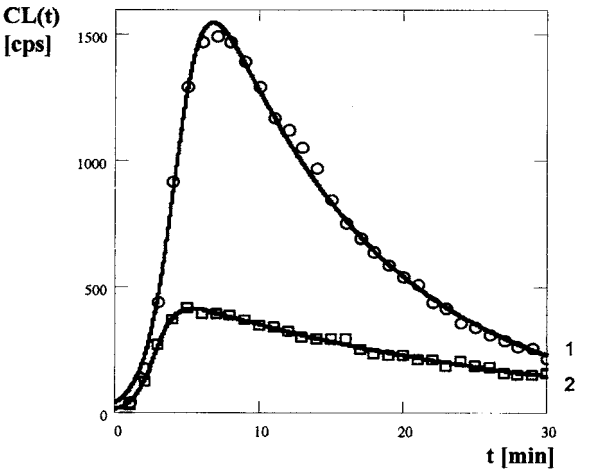

Fig. 17. The LE models for ChL of PMNs phagocytosing OZ at the presence of luminol; (1)or without (2) luminol [6];(1) $CL(t) = 3033\ \exp(-0.086t)/1 + \exp(4.356 - 0.990t)$,(2) $CL(t) = 538\ \exp(-0.043t)/1 + \exp(3.790 - 1.345t)$.

generation of light-emitters or oxidants. Also, the 93.6% decrease in k_3 means that the rate of the final step of the ChL reaction is reduced by DMSO.

4.2. Chemiluminescence of isolated human native or CB-treated PMNs stimulated with PMA

The effect of CB on human PMNs stimulated with PMA was described by Roschger et al. [6]. Time courses of ChL from native or CB-treated (8 μM) PMNs (5×10^6 cells/sample) stimulated with PMA (1 μM) are shown in Fig. 16. The model and reaction parameters are presented in Tables 1 and 2.

The ChL is stimulated by CB (the CL_m value increases by 67%, however, owing to $SD_r(k) =$ 144% this increase is insignificant (Section 2.3); the t_m and t_i values decrease insignificantly). Because of the 34.5% increase in the $(k_1[S]-k_2)/k_{-1}$ quotient one can conclude the shift of the reaction in Eq. (40) to its right side, i.e. to the higher light-emitter or oxidant generation. The 11.1% change in k_3 due to CB is insignificant.

4.3. Chemiluminescence of isolated human PMNs phagocytosing OZ without or with luminol

These processes were recorded by Roschger et al. [6]. Time courses of the ChL without or with luminol are presented in Fig. 17, and the model and reaction parameters are shown in Tables 1 and 2. The reagent concentrations: PMN, 5×10^6 cells/sample; OZ, a particle to cell ratio of 100:1; luminol, 16 nM [6].

The presence of luminol enhances the ChL (the CL_m value increases; the increase in the t_m and t_i values is insignificant). The $(k_1[S]-k_2)/k_{-1}$ quotient increases by 463.8%, which means the shift of the reaction in Eq. (40) to its right side, i.e. to the enhanced generation of light emitters. Simultaneously, k_3 increases by 100% in the presence of luminol.

4.4. Chemiluminescence of the t-BuOOH–RBC system with native or Immax A-treated RBCs

These ChL processes were described by Kochel and Sajewicz [5]. They are shown in Fig. 7, and their parameters are described in Tables 1 and 2. The reagent concentrations were as follows: RBCs, 2.5×10^5 cells ml^{-1}; Immax A, 2.67%; *t*-BuOOH, 2 mM; luminol, 0.2 mM [5].

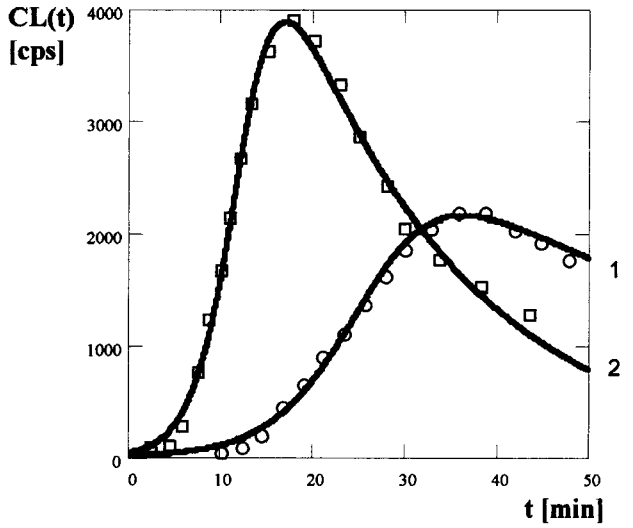

Fig. 18. The LE models for ChL of the L-DOPA autoxidation at pH 9.6 (1) or pH 8.8 (2) [4];(1) $CL(t) = 5118\ \exp(-0.021t)/1 + \exp(5.759 - 0.221t)$,(2) $CL(t) = 10\ 633\exp(-0.052t)/1 + \exp(5.506 - 0.444t)$.

The Immax A-treatment of RBCs stimulates the ChL in the *t*-BuOOH–RBC system (CL_m increases; the changes in the t_m and t_i values are insignificant). The $(k_1[S] - k_2)/k_{-1}$ quotient increases by 62.2%, which corresponds to the shift of the reaction in Eq. (40) to the higher light-emitter or oxidant generation. The 14.6% increase in k_3 caused by Immax A is insignificant.

4.5. Chemiluminescence of the L-DOPA autoxidation

Processes of autoxidation of L-DOPA in dependence on pH were described by Villablanca et al. [4]. The time courses of such autoxidative processes at pH 8.8 or 8.6 being fitted by the LE model are shown in Fig. 18. The model and reaction parameters are presented in Tables 1 and 2. The L-DOPA concentration was 0.4 μM [4].

The increase in pH from 8.6 to 8.8 stimulates the ChL of the L-DOPA autoxidation (CL_m increases; t_m and t_i decrease significantly). The $(k_1[S] - k_2)/k_{-1}$ quotient increases by 100.9%, which corresponds to the shift of the reaction in Eq. (40) to the higher light-emitter generation. The value of k_{-1} remains almost unchanged. The 147.6% increase in k_3 and the 55.0% decrease in C_{NL}^- are also caused by the increased pH.

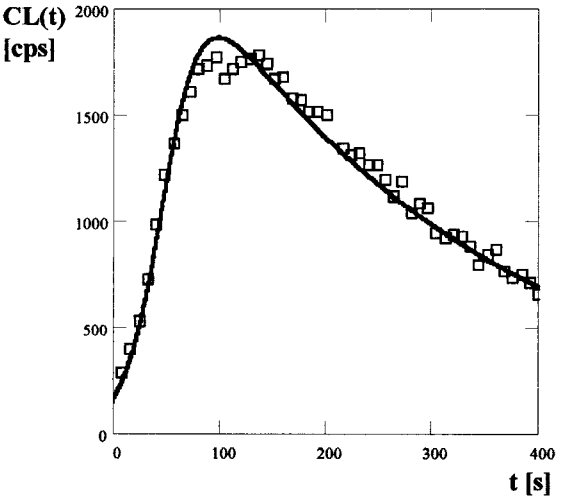

Fig. 19. The LE model for ChL of yeast intoxicated with 0.25% HCHO [11]: $CL(t) = 2804\ \exp(-0.0035t)/1 + \exp(2.746 - 0.055t)$.

4.6. Chemiluminescence of yeast intoxicated with formaldehyde

ChL process of yeast (Saccharomyces cerevisiae, TF-29 and TF-32 strains) intoxicated by formal-

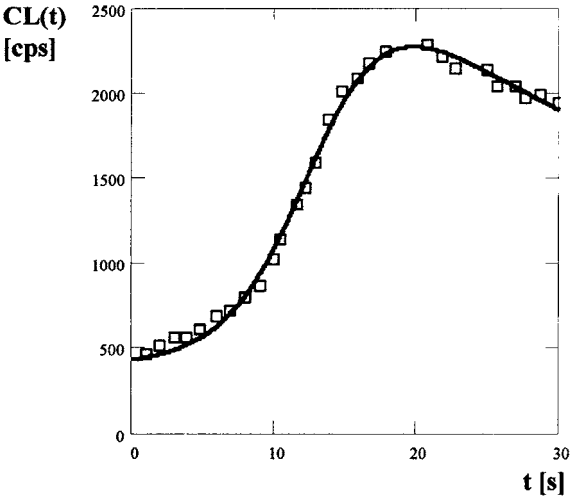

Fig. 20. The LE model for ChL of ferrous ion-treated bull spermatozoa [12]:$CL(t) = 3716\ \exp(-0.030t)/1 + \exp(4.645 - 0.355t) + 400$. The background emission of 400 cps is regarded.

dehyde (HCHO) (0.25%) was recorded by Godlewski et al. [11]. Data points for this process together with corresponding LE model are presented in Fig. 19. In Tables 1 and 2 the model's and reaction parameters are given.

4.7. Chemiluminescence of ferrous ion-treated bull spermatozoa

Ezzahir et al. [12] recorded a process generated by ferrous ion-treated (5×10^{-4} M) bull spermatozoa cells separated from seminal plasma and incubated in water. This process and its LE model are presented in Fig. 20, whereas the LE model's and reaction parameters are given in Tables 1 and 2.

4.8. Chemiluminescence of luminol oxidised in the Fenton reaction

This process generated in a system composed of luminol (10 μM), hydrogen peroxide and ferrous ions (2.5 μM) was recorded by Schiller et al. [7]. Process data points and the LE model are presented in Fig. 13. The LE model's and reaction parameters are presented in Tables 1 and 2.

From a viewpoint of the hypothesis of the two-pathway transformation of luminol, which was proposed by Schiller et al. [7], it would be valuable to compare the LE and DLE models (Section 2.4) constructed for more dense photon-counting time series composed of a greater amount of data points possibly recorded at a shorter counting time. Then, it would be possible to distinguish the LE and DLE models, thus to confirm or reject on the basis of the ChL kinetics the hypothesis of the two-pathway transformation which cannot be done at the present.

5. Concluding remarks

A new model for the ChL kinetics was constructed starting from the analysis of the ChL time course, then characterised and applied to several ChL processes produced by different biosystems. This model, called a LE one, was shown to fit successfully with these ChL processes and replace an inadequate two-exponential model. Moreover, the LE model was shown to correspond to a second-order dynamic system, variables of which take part in the reversible autocatalytic reaction, in which light-emitters are generated, followed by reactions of their mutual transformation and a radiation decay.

The proposed LE model can be also applied to non-chemiluminescent processes which contain two intermediate reagents and a negative feedback loop.

References

[1] A. Cohen, Biomedical signal processing, in: Time and Frequency Domains Analysis, vol. I, CRC Press, Boca Raton, 1988.
[2] B. Kochel, W. Sajewicz, Bull. Math. Biol. 59 (1997) 897.
[3] B. Kochel, W. Sajewicz, Toxicol. Lett. Suppl. 1/78 (1995) 48.
[4] M. Villablanca, G. Indig, D. Slawinska, J. Slawinski, J. Biolum. Chemilum. 3 (1989) 181.
[5] B. Kochel, W. Sajewicz, Report 14/2001, Immunotherapy Central Europe, Wrocław.
[6] P. Roschger, W. Graninger, H. Klima, J. Biolum. Chemilum. 5 (1990) 171.
[7] J. Schiller, J. Arnhold, J. Schwinn, H. Sprinz, H. Brede, K. Arnold, Free Rad. Res. 30 (1999) 45.
[8] J. Slawinski, Metody badania slabych emisji fotonowych z ukladow biologicznych, in: J. Twardowski (Ed.), Biospektroskopia 3, PWN, Warszawa, 1989, p. 107.
[9] B. Kochel, Experientia 48 (1992) 1059.
[10] B. Kochel, U.S. Patent 5849196, 1998.
[11] M. Godlewski, Z. Rajfur, A. Ezzahir, D. Sitko, M. Krol, Influence of environmental conditions on the luminescence from Saccharomyces cerevisiae, in: B. Jezowska-Trzebiatowska, B. Kochel, J. Slawinski, W. Strek (Eds.), Biological Luminescence, World Scientific, Singapore, New Jersey, London, Hong Kong, 1990, p. 182.
[12] A. Ezzahir, M. Godlewski, T. Kwiecinska, D. Sitko, J. Slawinski, B. Szczesniak-Fabianczyk, A. Laszczka, ABC 2/3 (1992) 139.